Cell Reports, Volume *22*

Supplemental Information

SynDIG4/Prrt1 Is Required for Excitatory Synapse Development and Plasticity Underlying Cognitive Function

Lucas Matt, Lyndsey M. Kirk, George Chenaux, David J. Speca, Kyle R. Puhger, Michael C. Pride, Mohammad Qneibi, Tomer Haham, Kristopher E. Plambeck, Yael Stern-Bach, Jill L. Silverman, Jacqueline N. Crawley, Johannes W. Hell, and Elva Díaz

SUPPLEMENTAL FIGURES AND LEGENDS

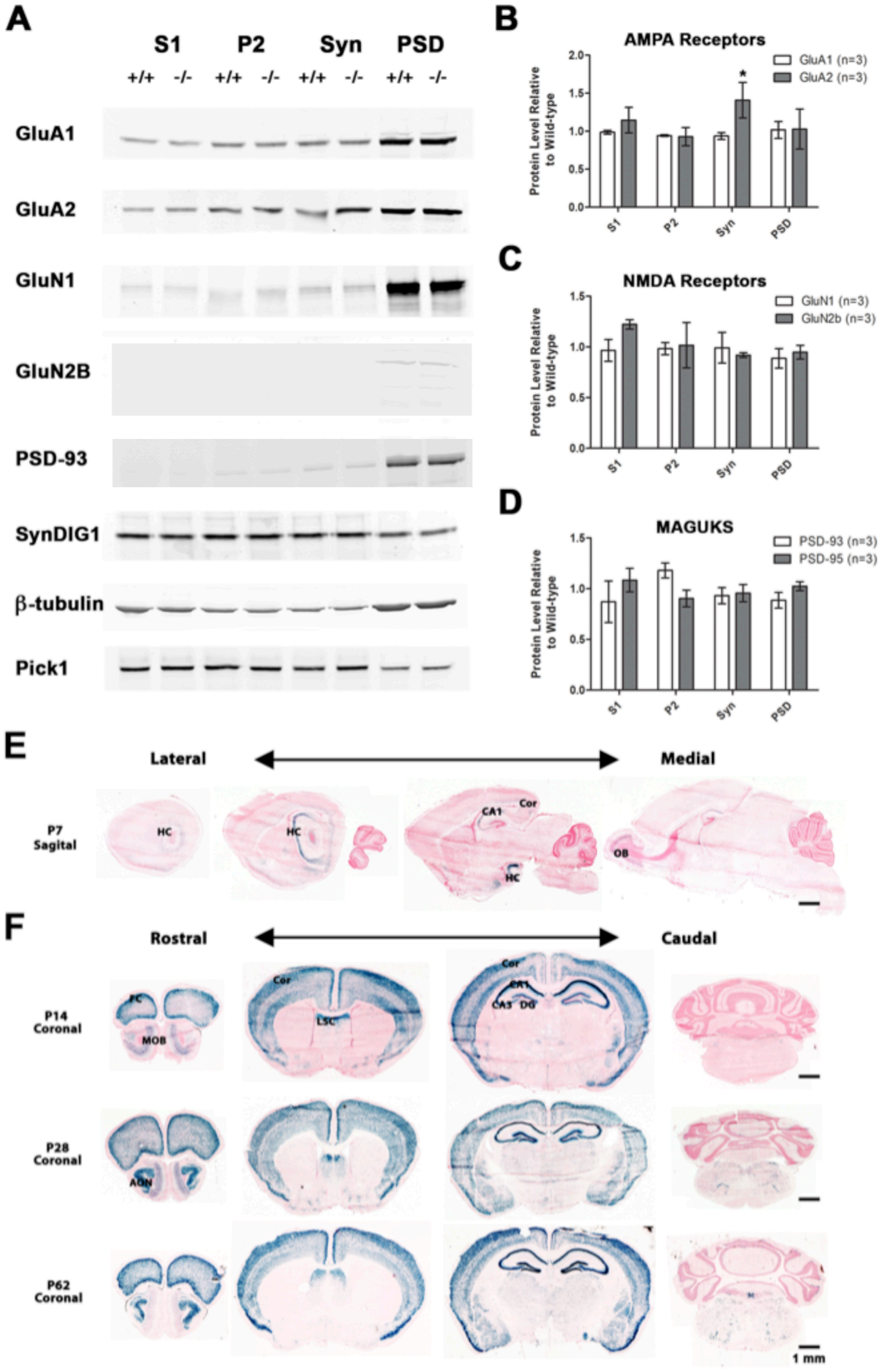

Figure S1. SynDIG4 deficient synapses have unchanged relative protein levels, Related to Figure 2.

(A) Representative immunoblots of biochemical fractions (10 µg protein loaded per lane) isolated from wild-type (+/+) and *SynDIG4*$^{-/-}$ homozygous mutant P14 mouse brain tissue showing levels of GluA1, GluA2, GluN1, GluN2B, PSD-93, SynDIG1, β-tubulin, and Pick-1 present in the postnuclear supernatant (S1), membrane pellet (P2), synaptosomal (Syn), and postsynaptic density (PSD) enriched fractions.

(B-D) Bar charts depicting the ratio of *SynDIG4*$^{-/-}$ homozygous mutant protein relative to wild-type levels of AMPA receptor subunits (B), NMDA receptor subunits (C), and PSD-93 and PSD-95 (D) in the PSD enriched fractions. Data are the average of three independent biochemical fractionation experiments; each experiment utilized 4-6 mouse forebrains of each genotype. Similar results were obtained with adult *SynDIG4*$^{-/-}$ and WT littermates (not shown). Error bars, ± standard error of the mean (SEM). Significance is indicated as: $*p < 0.05$.

(E) Sagittal sections from P7 *SynDIG4*$^{-/-}$ mice show β-gal reporter activity (blue) in the CA1 region of the hippocampus (HC) and within the olfactory bulb (OB).

(F) Coronal sections of P14, P28, and P62 mutant mouse brains show β-gal expression in frontal cortex (FC), main olfactory bulb (MOB), neocortex (Cor), caudal portion of the lateral septal nucleus (LSC), anterior olfactory nucleus (AON), and CA1, CA3, and dentate gyrus (DG) regions within the hippocampus.

All sections are counterstained with nuclear fast red. Some images are composites combining multiple individual images into one apparent photograph. Scale bar, 1 mm.

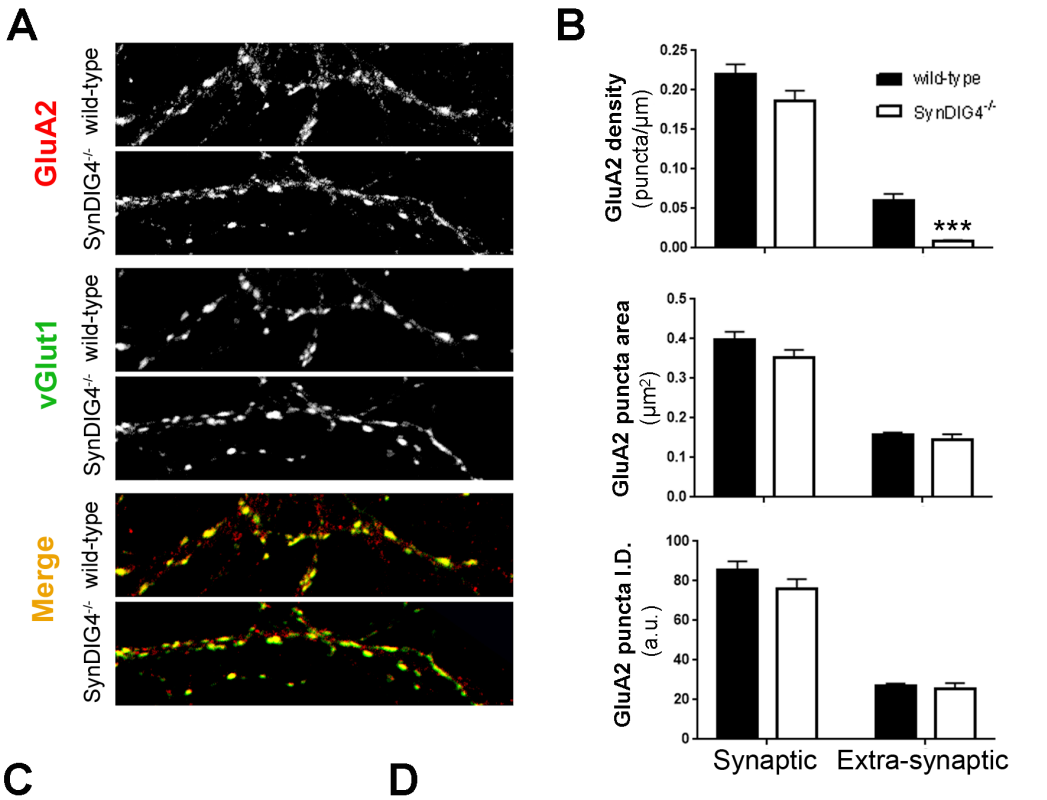
A
GluA2
vGlut1
Merge
wild-type
SynDIG4-/-
B
GluA2 density (puncta/µm)
wild-type
SynDIG4-/-
***
GluA2 puncta area (µm2)
GluA2 puncta I.D. (a.u.)
Synaptic
Extra-synaptic

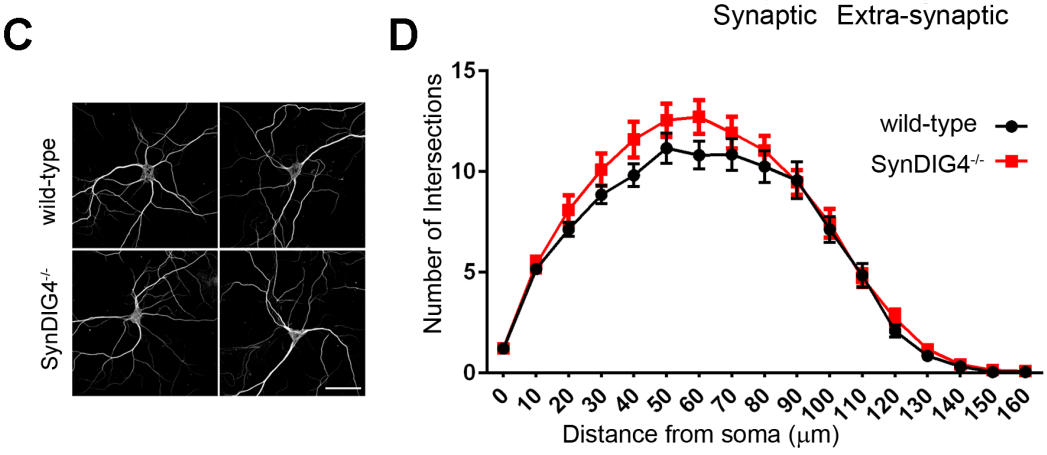
C
wild-type
SynDIG4-/-
D
Number of Intersections
wild-type
SynDIG4-/-
Distance from soma (µm)

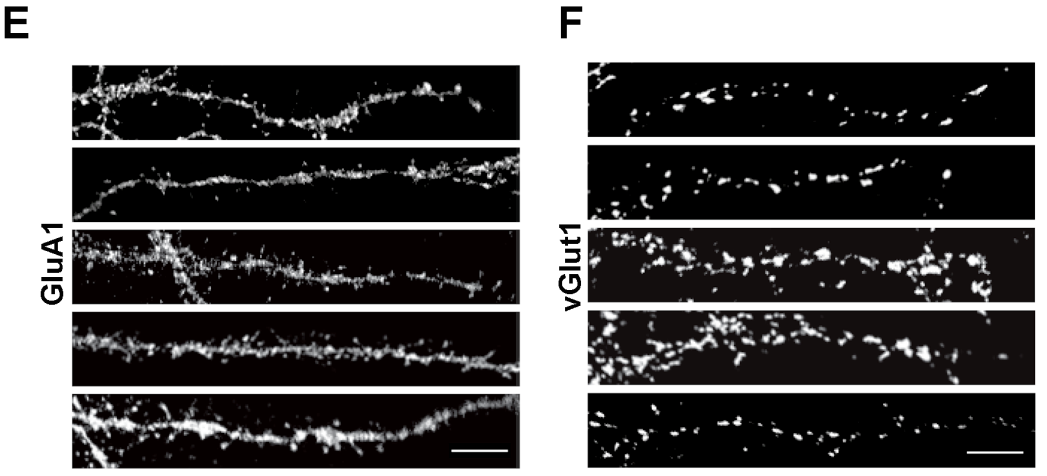
E
GluA1
F
vGlut1

Figure S2. Loss of SynDIG4 has no significant effect on synaptic GluA2 or dendrite complexity, Related to Figure 2.

(A) Representative images of wild-type and *SynDIG4*$^{-/-}$ dissociated hippocampal neurons at 14 DIV, stained with GluA2 and vGlut1.

(B) Graphs depict quantification of synaptic (overlap with vGlut1) or extrasynaptic (no overlap with vGlut1) GluA2 puncta density, puncta size and puncta Integrated Density (I.D.); Data are averaged from two independent experiments; n = 24-25 cells per genotype, per experiment; three dendrites per cell were selected for analysis.

(C) Representative neurons used in Sholl analysis stained with antibody against Map2b. Scale bar = 50 μm.

(D) Sholl analysis shows no significant difference in dendrite complexity (measured as the number of intersections at a defined radius from the soma) in wild-type vs *SynDIG4*$^{-/-}$ neurons.

(E-F) Representative dendritic stretches of dissociated rat hippocampal neurons at 14 DIV, stained separately for either GluA1 (E) or vGlut1 (F) and Alexa488- and Cy5-conjugated secondary antibodies. Note that GluA1 immunostaining is both punctate and diffuse, and can be clearly visualized in both dendritic spines and shafts while vGlut1 immunostaining labels distinct punctate structures in contact with the dendritic shaft, indicative of a pre-synaptic input. Five representative dendrite stretches were chosen from 10 different cells per condition/staining. Scale bar = 10 μm.

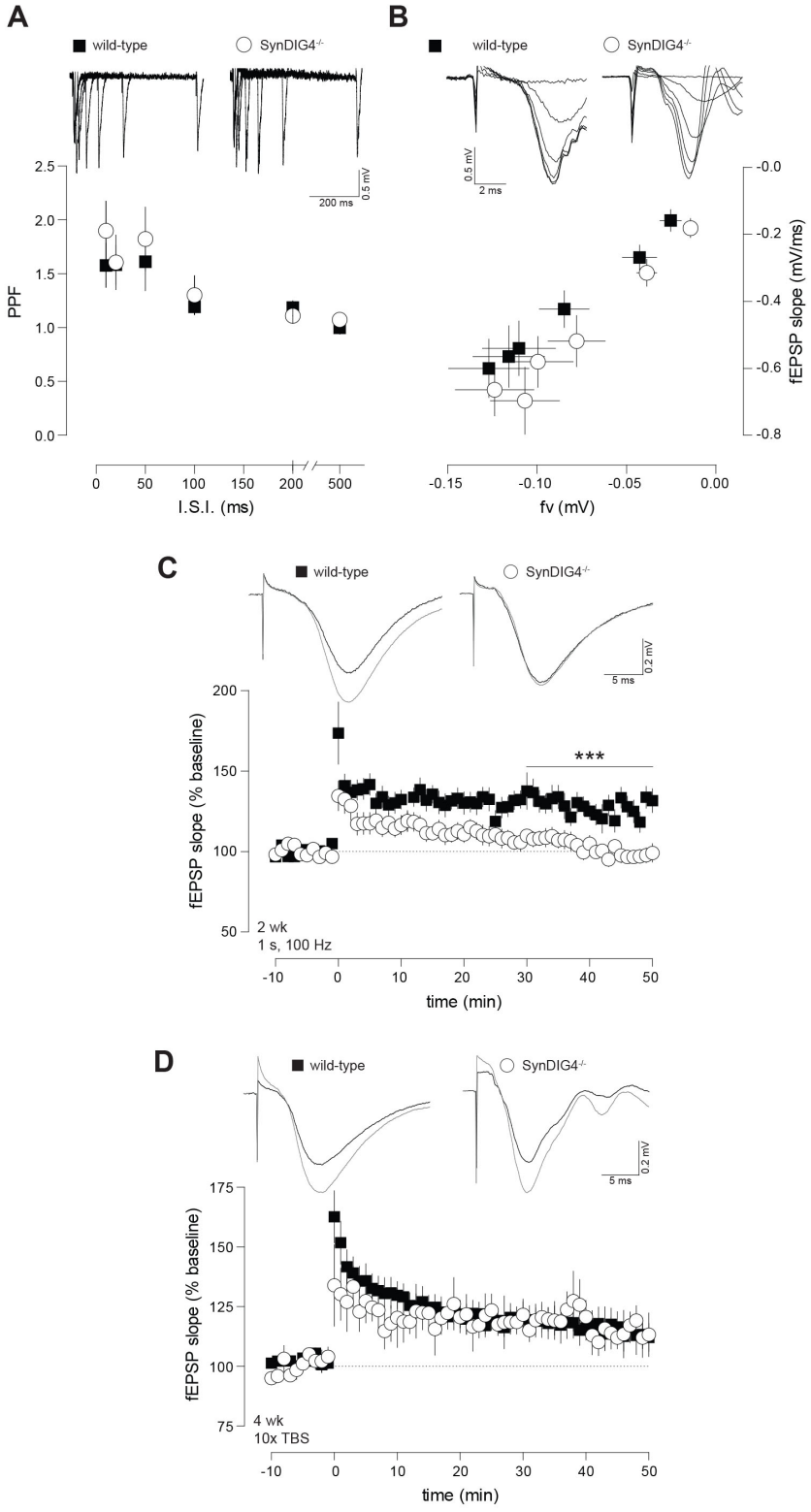
A
wild-type
SynDIG4-/-
200 ms
0.5 mV
PPF
I.S.I. (ms)
B
wild-type
SynDIG4-/-
0.5 mV
2 ms
fEPSP slope (mV/ms)
fv (mV)
C
wild-type
SynDIG4-/-
0.2 mV
5 ms
fEPSP slope (% baseline)
***
2 wk
1 s, 100 Hz
time (min)
D
wild-type
SynDIG4-/-
0.2 mV
5 ms
fEPSP slope (% baseline)
4 wk
10x TBS
time (min)

Figure S3. Synaptic transmission and plasticity properties in *SynDIG4*$^{-/-}$ mice, Related to Figure 3.

(A-B) Schaffer-collateral fEPSP were recorded from acute forebrain slices of 8 – 12 week-old wild-type and *SynDIG4*$^{-/-}$ mice.

(A) Paired-pulse facilitation (PPF) was not different between wild-type (n = 15) and *SynDIG4*$^{-/-}$ (n = 16) for all inter-stimulus intervals (I.S.I.). Traces from representative recordings shown on top (wild-type: 10 ms: 1.6 ± 0.2 mV, 20 ms: 1.6 ± 0.2 mV, 50 ms: 1.6 ± 0.3 mV, 100 ms: 1.2 ± 0.1 mV, 200 ms: 1.2 ± 0.1 mV, 500 ms: 1.0 ± 0.1 mV, n = 15; SynDIG4$^{-/-}$: 10 ms: 1.9 ± 0.3 mV, 20 ms: 1.6 ± 0.3 mV, 50 ms: 1.8 ± 0.3 mV, 100 ms: 1.3 ± 0.2 mV, 200 ms: 1.1 ± 0.1 mV, 500 ms: 1.1 ± 0.1 mV, n = 16).

(B) Averaged fEPSP slope was plotted against averaged fiber volley amplitude (fv) for all signals elicited by increasing stimulation strengths. No difference was observed between wild-type (-0.025 ± 0.006 mV / -0.16 ± 0.03 mV/ms, -0.043 ± 0.010 mV / -0.27 ± 0.04 mV/ms, -0.085 ± 0.014 mV / -0.42 ± 0.05 mV/ms, -0.110 ± 0.020 mV / -0.54 ± 0.08 mV/ms, -0.116 ± 0.020 mV / -0.56 ± 0.09 mV/ms, -0.127 ± 0.022 mV / -0.60 ± 0.09 mV/ms ;n = 14) and *SynDIG4*$^{-/-}$ (-0.014 ± 0.003 mV / -0.18 ± 0.03 mV/ms, -0.039 ± 0.006 mV/ -0.18 ± 0.03 mV/ms, -0.078 ± 0.016 mV / -0.52 ± 0.08 mV/ms, -0.100 ± 0.020 mV / -0.58 ± 0.08 mV/ms, -0.107 ± 0.019 mV / -0.70 ± 0.10 mV/ms, -0.124 ± 0.022 mV, -0.66 ± 0.08 mV/ms; n = 8).

(C) Schaffer-collateral fEPSP were recorded from acute forebrain slices of two week-old mice. The 1 sec, 100 Hz tetanus elicits robust LTP in wild-type but not *SynDIG4*$^{-/-}$ mice (wild-type: 128 ± 7, n = 10, $p < 0.001$ vs baseline; *SynDIG4*$^{-/-}$: 100 ± 4, n = 15, $p < 0.001$ vs WT; 1-way ANOVA with Bonferroni's Test between baseline and tetanized and between tetanized).

(**D**) Schaffer-collateral fEPSP were recorded from acute forebrain slices of 4 week-old mice. Theta-burst stimulus (TBS) led to robust LTP in *SynDIG4*$^{-/-}$ mice not different from control (wild-type: 115 ± 6, n = 5, $p < 0.05$ t-test vs baseline; *SynDIG4*$^{-/-}$: 115 ± 6, n = 4, $p < 0.001$ t-test vs baseline).

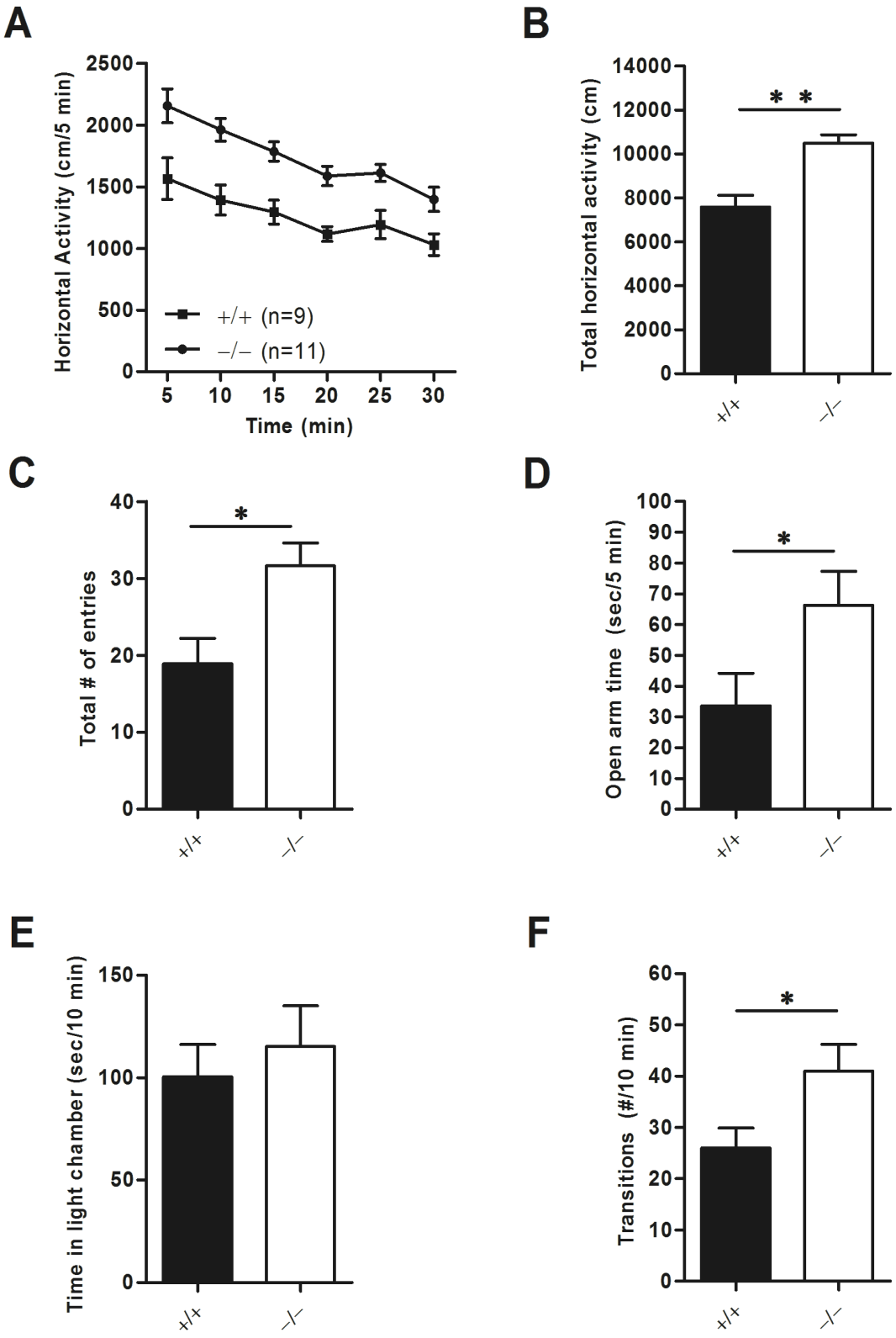
A
Horizontal Activity (cm/5 min)
2500
2000
1500
1000
500
0
+/+ (n=9)
–/– (n=11)
5
10
15
20
25
30
Time (min)
B
Total horizontal activity (cm)
14000
12000
10000
8000
6000
4000
2000
0
* *
+/+
–/–
C
Total # of entries
40
30
20
10
0
*
+/+
–/–
D
Open arm time (sec/5 min)
100
90
80
70
60
50
40
30
20
10
0
*
+/+
–/–
E
Time in light chamber (sec/10 min)
150
100
50
0
+/+
–/–
F
Transitions (#/10 min)
60
50
40
30
20
10
0
*
+/+
–/–

Figure S4. Additional behavioral phenotypes of *SynDIG4*$^{-/-}$ mice, Related to Figure 4.

(A) Locomotor activity of *SynDIG4*$^{-/-}$ mice is significantly higher than wild-type mice.

(B) Total horizontal distance traveled in (A) is significantly higher in *SynDIG4*$^{-/-}$ mice than wild-type mice.

(C) In the elevated plus-maze (EPM), the total number of entries is significantly higher in *SynDIG4*$^{-/-}$ mice than wild-type mice.

(D) Time spent in the open arms of the EPM is significantly higher in *SynDIG4*$^{-/-}$ mice than wild-type mice.

(E) In the light↔dark (L↔D) box, the time spent in the light chamber did not differ between *SynDIG4*$^{-/-}$ mice and wild-type mice.

(F) In the L↔D box, the number of transitions was significantly higher in *SynDIG4*$^{-/-}$ mice than wild-type mice.

The significant differences observed in the EPM and L↔D tests could be a consequence of the elevated exploratory locomotor activity of the *SynDIG4*$^{-/-}$ animals.

For all experiments: wild-type, n = 9; *SynDIG4*$^{-/-}$, n = 11; Significance is indicated as: *$p < 0.05$; **$p < 0.01$.

SUPPLEMENTAL TABLES

Table S2. Primary Antibody Information, Related to Figures 2, S1, S2.

Target	Source	Catalog #	Species	Figure
β-actin	Abcam	ab8224	rabbit polyclonal	2
β-tubulin	Millipore	05-661	mouse monoclonal	S1
GluA1	Millipore	AB1504	rabbit polyclonal	2, S1
GluA2	NeuroMab	75-002	mouse monoclonal	S1, S2
GluN1	BD Biosciences	556308	mouse monoclonal	S1
GluN2B	NeuroMab	75-097	mouse monoclonal	S1
Map2b	Sigma	M4403	mouse monoclonal	S2
Pick1	NeuroMab	73-040	mouse monoclonal	S1
PSD-93	NeuroMab	75-057	mouse monoclonal	S1
PSD-95	NeuroMab	75-028	mouse monoclonal	2
Synaptophysin	Synaptic Systems	101011	mouse monoclonal	2
SynDIG1	NeuroMab	75-251	mouse monoclonal	S1
SynDIG4 (NG5.1)	Gift from A.B. Smit	custom	rabbit polyclonal	2
vGlut1	Millipore	AB5905	guinea pig polyclonal	2, S2

Table S3. Level and area of total GluA1 and GluA2 that does not overlap with vGlut1, Related to Figure 2.

	genotype	results	n	Statistics
		Total GluA1 per µm dendrite	Cells, dendrites	
	wild-type	Summed levels: 404.29±32 Summed area: 0.0336±0.0026	25,125	
	SynDIG4$^{-/-}$	Summed levels: 205.43±18 Summed area: 0.0177±0.0015	25,125	p = 2.2141E-07 vs wild-type p = 4.4082E-07 vs wild-type
		Total GluA2 per µm dendrite	Cells, dendrites	
	wild-type	Summed levels: 520.10±50.21 Summed area: 0.0313±0.003	25, 69	
	SynDIG4$^{-/-}$	Summed levels: 211.23±20.69 Summed area: 0.0123±0.001	25, 74	p = 1.5619E-07 vs wild-type p = 4.7565E-08 vs wild-type

Table S4. General health information for *SynDIG4*$^{-/-}$ and WT mice, Related to Figure 4.

Genotypes	**WT** N = 9	***SynDIG4* -/-** N = 11	***p*-value**
Body Weight	26.68±1.54	23.1±2.3	not significant (n.s.)
Body Temperature	36.34±0.23	36.38±0.168	n.s.
Fur quality (3 pt scale)	2	2	n.s.
Bald patches (%)	0%	0%	n.s.
Missing whiskers (%)	0%	0%	n.s.
Piloerection	0%	0%	n.s.
Body tone (3 pt scale)	2	2	n.s.
Limb tone (3 pt scale)	2	2	n.s.
Skin color (3 pt scale)	2	2	n.s.
Physical abnormalities	0%	0%	n.s.
Trunk curl (%)	100%	100%	n.s.
Wire hang (sec)	60±0	60±0	n.s.
Forepaw reach (%)	100%	100%	n.s.
Righting reflex (%)	100%	100%	n.s.
Corneal (%)	100%	100%	n.s.
Whisker twitch (%)	100%	100%	n.s.
Ear twitch (%)	100%	100%	n.s.
Auditory startle (%)	100%	100%	n.s.
Struggle/vocalization (%)	33.33%	18.18%	n.s.
Dowel biting (3 pt scale)	2.33	2.27	n.s.

EXPERIMENTAL PROCEDURES

Animals

Frogs. Xenopus laevis frogs (females, age 1-3 years old) were used as a source for oocytes for heterologous expression and outside-out patch-clamp electrophysiological recordings. Maintenance of the frogs and extraction of oocytes were performed in accordance with the National Institutes of Health (NIH) guidelines for the Care and Use of Laboratory Animals and the Israeli law for animal experimentation and were approved by the Institutional Animal Care and Use Committee (IACUC) of the Hebrew University of Jerusalem.

Mice. Mouse embryonic stem (ES) cells with a targeted deletion of the SynDIG4 locus were obtained from the Mouse Biology Program (MBP) at UC Davis. The mutant allele [*Prrt1*$^{tm1(KOMP)Vlcg}$] was generated by Velocigene as part of the trans-NIH Knock Out Mouse Project (KOMP), obtained from the KOMP Repository (www.komp.org) and maintained on C57BL/6 line. NIH grants to Velocigene at Regeneron Inc (U01HG004085) and the CSD Consortium (U01HG004080) funded the generation of gene-targeted ES cells for 8500 genes in the KOMP Program and archived and distributed by the KOMP Repository at UC Davis and CHORI (U42RR024244). The β-galactosidase (β-gal) and neomycin cassette ZEN-UB1 replaced the protein coding region of the *SynDIG4* locus leaving non-coding portions of exons 1 and 4 and β-gal expression driven by the SynDIG4 promoter. The day of birth is referred to as postnatal day 0 (P0). Wild-type (WT) controls are either littermates or are derived from separate homozygous crosses from a common lineage. Mutant mice are viable and fertile, exhibit Mendelian inheritance and do not exhibit any alterations in parameters of general health (Table S6). All mice were group-housed in a climate-controlled facility on a 12-hour light/dark cycle (lights on at 06:00), and food (Teklad 2918, Harlan) and water were available *ad libitum*. Corncob bedding with a handful of shredded paper and nestlets (Eco-Bedding™, FiberCore, Cleveland, OH) lined the cage bottom. *Rats.* Sprague Dawley timed pregnant rats were

purchased from Harlan. Rats were housed and maintained in the animal facility at UC Davis. The use and maintenance of animals were carried out according to the guidelines set forth by the NIH and approved by IACUC at UC Davis.

Antibodies and Reagents

All primary antibodies used in the present study are listed in Table S1. The following secondary antibodies were used: Alexa Fluor 488-conjugated secondary antibodies (Molecular Probes), Cy3- or Cy5-conjugated secondary antibodies (Jackson ImmunoResearch), IRDye-conjugated secondary antibodies (LiCOR), and HRP-conjugated secondary antibodies (Thermo Fisher Scientific).

PSD fractionation and immunoblotting

The rostral 2/3 of P14 mouse brains were homogenized by dounce homogenation in 0.32 M sucrose, 1 mM Tris pH 7.4, 1 mM $MgCl_2$ with protease inhibitors (leupeptin, aprotinin, pepstatin A, and phenylmethylsulfonyl fluoride). Lysate was spun 15 minutes at 1400 xg. Supernatant was collected and saved. The pellet was homogenized with more sucrose solution and large insoluble debris and the nuclear fraction were removed by centrifugation at 710 xg. The supernatants were pooled and an aliquot saved as the postnuclear supernatant (S1) fraction. The remaining S1 was centrifuged at 16000 xg, and the pellet collected as the membrane-enriched fraction (P2). The P2 fraction was resuspended in 0.32 M sucrose solution without $MgCl_2$ and layered over 0.85 M, 1.0 M, and 1.25 M sucrose gradients, spun at 40000 xg for 2 hours, and synaptosomal enriched fraction (Syn) was collected between 1.0/1.25 M gradients. Triton X-100 was added to Syn to a final concentration of 0.5% and incubated for 15 minutes at 4°C. The pellet was collected after 100000 xg spin for 30 minutes. The pellet was resuspended in sucrose buffer, placed over another sucrose gradient (1.0/1.5/2.0 M), centrifuged at 40000 xg for 2 hours, and second gradient layer collected between 1.5/2.0 M sucrose interface. This

fraction was exposed to Triton X-100 again and a final PSD pellet collected after centrifugation at 100000 xg for 1 hour, which was resuspended via sonication to obtain the PSD enriched fraction (PSD). Protein was quantified using a BCA assay (Thermo Fisher Scientific) and 10-20 μg of protein were run on 7-15% acrylamide gels, which were transferred to nitrocellulose membranes, stained with antibodies, and protein levels measured on an Odyssey® LICOR system. S1, P2, Syn and PSD fractions were normalized to β-actin and/or β-tubulin. *SynDIG4*$^{-/-}$ mutant fractions were divided by WT protein levels and student's t-test analyses revealed no statistically significant differences.

X-gal staining

Unfixed fresh mouse brains (ages P7, P14, P28, P62) were quickly frozen on dry ice in Optimal Cutting Temperature (OCT) medium and sectioned at 15-25 μm on a Leica cryostat. Sections were stained with X-gal (5-Bromo-4-chloro-3-indolyl-β-D-galactopyranoside; Roche).

Primary dissociated neuronal culture and Immunocytochemistry

Cell culture and Immunocytochemistry. Neurons from hippocampi of P1 WT and *SynDIG4*$^{-/-}$ mice littermates were dissociated individually in papain (Worthington) and plated at a density of 12,500 cells/cm^2. Neurons from hippocampi of embryonic day 18 (E18) WT rat embryos were dissociated with 2.5% trypsin (Life Technologies) and plated at a density of 5,500/cm^2. Neurons were grown on poly-L-lysine-coated glass coverslips media supplemented with B-27 and N2 (Thermo Fisher Scientific). Neurons were fixed in 4% formaldehyde at 14 days in vitro (DIV), permeabilized for 15 min in 0.1% Triton X-100, and blocked for 30 min in 3-10% bovine serum albumin (Life Technologies). Coverslips were incubated in primary antibody overnight at 4°C, secondary antibody at room temperature (RT) for 1 hr, and mounted onto glass slides using Flouromount-G (Southern Biotech).

Image acquisition. Images were acquired using a Zeiss LSM700 scanning confocal microscope or an Olympus Fluoview 1000, with a 63x/ 1.5 NA objective with identical settings for laser power, photomultiplier gain, and digital offset within each experiment. Settings were established such that no signal was observed with coverslips stained only with secondary antibodies. Imaging was performed blinded as to genotype.

Image analysis. All analyses were performed blind to genotype. Images were imported into ImageJ software for identification of representative stretches for quantitative analysis of synaptic puncta (colocalized with vGlut1) or extrasynaptic puncta (no colocalization with vGlut1), and addition of scale bars. Thresholds were established using a subset of images from each image set so that all puncta were included, and the average threshold was applied to the entire data set for quantitative analysis. A minimum size cutoff of 0.09 was applied to eliminate speckled background stain. For each cell, dendrites beyond the first branch point were selected for quantification. A mask was created for each channel, and colocalization was defined as any partially overlapping punctate structure. Synaptic AMPARs were identified as puncta colocalizing with vGlut1. Another mask was then created of the synaptic puncta, and was subtracted from the mask of total AMPAR puncta to create a mask representing "extrasynaptic AMPARs." These masks were used to measure puncta size and number of puncta, and were redirected to the original image for fluorescence quantification (Integrated Density, I.D.). Density was calculated by measuring the number of puncta per length of dendrite. For extrasynaptic levels and area, images were thresholded as described above. A mask was created for synapses (identified by the overlap of GluA and vGlut1 staining) and subtracted from the GluA image, leaving only extra-synaptic signal. No size cutoff was applied; therefore, all particles that passed the threshold were included in the analysis. The total greyscale levels and area were summed for the dendrite stretch, and normalized to dendrite length. Data were imported into GraphPad Prism 7.0 for statistical analysis and a two-tailed student's t-test was calculated. All data are shown as mean ± standard error of the mean (SEM). Significance levels are indicated

by asterisks: * $p \leq 0.5$, ** $p \leq 0.01$, *** $p \leq 0.001$. Signals were adjusted for all images by using linear adjustments of levels in Photoshop and figures assembled in Illustrator (Adobe Systems). All panels within a figure were treated identically. Data are presented as mean ± SEM.

Sholl analysis. The morphometric Sholl analysis was obtained from WT and *SynDIG4*$^{-/-}$ dissociated hippocampal neurons fixed and stained at 14 DIV with Map2b primary antibody. Dendrites were traced using the Fiji extension Simple Neurite Tracer, followed by Sholl analysis plugin. A series of concentric spheres (centered around the soma) were drawn with an intersection interval of 10 μm and the number of dendrites crossing each sphere was calculated and was plotted against the distance from the soma.

Statistical analysis. GraphPad Prism was used to calculate a repeated measure ANOVA with genotype as the between group factor and distance from soma as the repeated measure factor. Holm-Sidak multiple comparison test was used to compare means of a defined distance to soma between different genotypes. All tracings and analyses were blinded to genotype. Data are presented as mean ± SEM.

Electrophysiology

Heterologous expression in oocytes and outside-out patch-clamp recordings. Stage V–VI *Xenopus laevis* oocytes were prepared and injected with cRNA as previously described (Priel et al., 2006) prepared from pGEMHE plasmids carrying GluA1 (Q/flip), GluA2 (R/flip), HA-tagged SynDIG4 and EGFP-tagged TARPγ8. For giant outside-out patch recordings the vitelline membrane was removed using forceps. Recordings were performed at 17^{o}C, at membrane potential of -120 mV, using Axopatch 200B amplifier connected to digidata1322A and pCLAMP10.2 (Axon Instruments, Foster City, CA) and analyzed using ClampFit10.2 and Origin 8 (Origin Lab, Northampton, MA) software. For rapid solution exchanges, a double-barrel glass (theta tube) mounted on a piezoelectric translator (Burleigh, Fishers, NY) was used as

previously described (Priel et al., 2005). Patch electrodes were fabricated from borosilicate glass with a low resistance of 0.3-0.7 MΩ. AMPAR deactivation and desensitization were measured by applying glutamate (10 mM) for 1 ms and 500 ms, respectively. Recovery from desensitization was estimated with the two-pulse protocol in which a constant 100 ms application of glutamate (10 mM) was followed by a 100 ms test pulse applied at different time intervals. AMPAR-current deactivation and desensitization were fitted with two exponentials and the weighted tau (τ_w) was calculated as $\tau_w = (\tau f \times af) + (\tau s \times as)$, where af and as are the relative amplitudes of the fast (τf) and slow (τs) exponential component. *Statistical analysis.* Significance was compared with AMPAR expressed alone (*) or with AMPAR+TARPγ8 ($); *p*-value (one-way ANOVA): */$ < 0.05; **/$$ < 0.01; ***/$$$ < 0.001; ns, not significant.

Preparation of hippocampal slices. Mice were decapitated and brains put into ice cold dissection buffer (composition in mM: 127 NaCl, 1.9 KCl, 26 $NaHCO_3$, 1.2 KH_2PO_4, 10 dextrose, 2 $MgSO^4$, and 1.1 $CaCl_2$, saturated with 5% CO_2 and 95% O_2, final pH 7.4). The cerebellum was removed and forebrain slices were cut with a vibratome (Leica VT 1000A) and subsequently maintained in artificial cerebrospinal fluid (ACSF, in mM: 127 NaCl, 26 $NaHCO_3$, 1.2 KH_2PO_4, 1.9 KCl, 2.2 $CaCl_2$, 1 $MgSO_4$ and 10 D-glucose oxygenated with 95% O_2 plus 5% CO_2, final pH 7.4) for 1 hour at 30 °C and then for up to 5 hours at room temperature.

Field EPSP recordings in hippocampal slices. Field EPSPs (fEPSPs) were recorded as previously described (Matt et al., 2011). 400 µm thick slices from 8-12 week old mice were transferred into a submerged type recording chamber constantly perfused with oxygenated ACSF supplemented with 5 µM Bicuculline (Tocris) at 30°C. fEPSPs were recorded in the Schaffer collateral pathway with stimulation and recording electrodes positioned within the stratum radiatum near the CA3 region and recording electrodes in the CA1 region. fEPSPs were recorded using ACSF-filled glass pipettes (2-3 MΩ), amplified with an Axopatch 2B amplifier (Molecular Devices, CA), digitized at 10 kHz with a Digidata 1320A (Molecular Devices) and

recorded with Clampex 9 (Molecular Devices). Stimuli (100 μs) were delivered through a concentric bipolar electrode (TM53CCINS, WPI). The same intensity was used during baseline recording (0.067 Hz) and induction of LTP by tetanic stimulation. Tetanus paradigm consisted of 100 stimuli given at 100 Hz (1 sec). Theta-burst consisted of 10 bursts consisting of 4 stimuli at 100 Hz with a burst frequency of 5 Hz. The baseline was determined by the average of fEPSP initial slopes from the 10-minute period immediately before the tetanus. The level of LTP was determined by the average of fEPSP initial slopes from the period between 30 and 50 minutes after the tetanus. The same slices used for LTP recordings were used to record input-output relation (IOR) for stimulus intensities of 0.1 – 0.6 mA and paired-pulse facilitation (PPF) for inter-stimulus intervals of 10 ms, 20 ms, 50 ms, 100 ms, 200 ms, and to 500 ms (same stimulation strength as LTP recordings). For each data point, four individual traces were averaged. Data were analyzed and processed using Clampfit 9 and Microsoft Excel. Statistics and visualization were performed with GraphPad Prism. Results between genotypes were statistically compared using one-way ANOVA and Bonferroni's Multiple Comparison Test to compare baseline levels vs post-tetanus for both genotypes as well as post-tetanus levels between genotypes.

Whole-cell patch-clamp recording. 350 μm thick forebrain slices from P12-15 mice, prepared as described for extracellular recordings, were transferred into a submerged recording chamber constantly perfused with oxygenated ACSF supplemented with 5 μM Bicuculline at room temperature. Hippocampal pyramidal neurons were visually identified using an Olympus BX50WI upright microscope and an Olympus LumPlanFL 40x water-immersion objective with IR-DIC contrast through a Hamamatsu C2400 CCD camera. Patch micropipettes (2.5 – 5 MΩ) were filled with intracellular solution (in mM: 125 $CsMeSO_3$, 2.5 CsCl, 7.7 TEA, 4 Mg-ATP, 0.3 Na_2-GTP, 20 HEPES, 8 NaCl, 0.2 EGTA; pH 7.2) containing 5 mM QX-314 (Sigma) to prevent action potential firing. All patch-clamp recordings were made in whole-cell configuration using Clampex 9 to control an Axopatch 200B patch-clamp amplifier (Molecular Devices) through a Digidata 1322A digitizer. Cell capacitance and series resistance were monitored but not

compensated throughout experiments. Stimulation electrode was positioned in the stratum radiatum. Stimulus intensity was set to evoke 50% EPSC amplitude at a holding potential of -70 mV. Test pulses were given every 15 sec. After 5 min of baseline (no more than 8 min after break-in) cells were depolarized to 0 mV. After waiting 150 sec for accommodation, 180 pulses were applied with 2 Hz (90 sec) before the holding potential was switched back to -70 mV and test pulses resumed after 15 sec for 30 min. Signals were sampled at 10 kHz using a 2 kHz low-pass filter. LTP was determined using Clampfit 10 as the average EPSC amplitude recorded 15 – 30 min after pairing normalized to the average baseline EPSC. Results between genotypes were statistically compared using one-way ANOVA and Bonferroni's Multiple Comparison Test to compare baseline vs LTP for both genotypes as well as LTP between genotypes. For mEPSC recordings the extracellular ACSF was supplemented with 50 mM sucrose, 1 µM TTX (Tocris), and 5 µM Bicuculline. Cells were held at -70 mV and miniature events were sampled for up to 30 min at 2 kHz and filtered with a 1 kHz low-pass filter. Events were identified using Clampfit's inbuilt template-based event detection function. All events from one individual cell were averaged. Per-cell averages were used for statistical comparison between genotypes using unpaired t-tests. Analysis was performed using Microsoft Excel and GraphPad Prism.
Statistical analysis. GraphPad Prism 4.0 was used for statistical analysis. All data are shown as mean ± SEM. Significance levels are indicated by asterisks: n.s. not significant, * $p \leq 0.5$, ** $p \leq 0.01$, *** $p \leq 0.001$. Unless stated otherwise data were compared using one-way ANOVA and Bonferroni's Multiple Comparison Test against selected columns.

Behavior studies

Founder mice generated on a C57BL/6N genetic background were backcrossed four times (N4) onto the C57BL/6J strain to remove the *rd8* mutation (Mattapallil et al., 2012). Heterozygous N4 mice devoid of the *rd8* mutation were then intercrossed to produce WT and mutant (*SynDIG4*$^{-/-}$)

mice for behavioral experiments. Both males and females (ages 3-5 months) were used for behavioral testing at age (WT: 5 males and 4 females; *SynDIG4*$^{-/-}$: 3 males and 8 females). As no sex differences were detected on the cognitive scores, results from males and females were combined within genotype, to reach N = 9 WT, N = 11 *SynDIG4*$^{-/-}$. Mice were bred and housed on the UC Davis main campus and then transferred to the Sacramento campus for behavioral testing after a one-week habituation period. Researchers at the Sacramento facility were blinded to the genotype of the mice until after all behavioral experiments had been performed.

Morris Water Maze. Hippocampal-dependent spatial navigation learning and memory was evaluated using a standard Morris water maze (Vorhees and Williams, 2006). The Morris water maze was a 120 cm circular pool, filled 45 cm deep with water (24^{o}C) made opaque with non-toxic white paint (Crayola). External cues to aid spatial navigation included a prominent sink, computer, water temperature regulator with hose, a large black X on the wall and a yellow paper lantern hung from the ceiling. Trials were video recorded and scored by automated software (Noldus Ethovision, Wageningen, Netherlands) for measures including latency to find the hidden platform, total distance traveled, and swim speed. Mice were trained in the hidden platform version of the Morris water maze consistent with methods standard in the literature (Vorhees and Williams, 2006; Yang et al., 2012). Briefly, each mouse was placed into the water maze, facing the wall, in one of four possible quadrant locations, which differed pseudo-randomly by training day. Mice were given 60 seconds to find the hidden platform. If a subject mouse was unable to find the platform by the end of 60 seconds, it was gently guided to the platform and allowed to rest for ~10 seconds between trials. The hidden platform was in the same location, in the same quadrant, on each training day. Acquisition training consisted of four trials per day for five days. Trials were given sequentially, with an approximately 10 second platform rest interval. Mice were placed under infrared heating lamps after the last trial each day to prevent hypothermia. Acquisition was assessed daily until the WT group reached a latency criterion of <15 seconds to reach the hidden platform. Approximately 3 hours after the last training trial, the

platform was removed and mice underwent a 60 second probe trial to determine the amount of time spent exploring the target quadrant and the number of times the animal crossed the previous platform location and corresponding pseudo-platform locations in each quadrant.

Novel object recognition. The novel object recognition test was conducted in opaque matte white (P95 White, Tap Plastics, Sacramento, CA) open field arenas (40 cm x 60 cm x 23 cm), using methods similar to those previously described (Silverman et al., 2013a; Silverman et al., 2013b; Yang et al., 2012). The experiment consisted of three sessions, a 30 min exposure to the open field arena, a 10 min familiarization session and a 5 min recognition test. On day 1, each subject was habituated to a clean empty open field arena for 30 min. Twenty four hours later each subject was returned to the open field arena for the habituation phase, for 10 min. The mouse was then removed from the open field and placed in a clean temporary holding cage for approximately 2 min. Two identical objects were placed in the arena. Each subject was returned to the open field in which it had been habituated, and allowed to freely explore for 10 min. After the familiarization session, subjects were returned to their holding cages, which were transferred from the testing room to a nearby holding area. The open field was cleaned with 70% ethanol and let dry. One clean familiar object and one clean novel object were placed in the arena, where the two identical objects had been located during in the familiarization phase. Sixty minutes after the end of the familiarization session, each subject was returned to its open field for a 5 min recognition test, during which time it was allowed to freely explore the familiar object and the novel object. The familiarization session and the recognition test were videotaped and scored with Ethovision XT video tracking software (Version 9.0, Noldus Information Technologies, Leesburg, VA). Object investigation was defined as time spent sniffing the object when the nose was oriented toward the object and the nose-object distance was 2 cm or less. Recognition memory was defined as spending significantly more time sniffing the novel object than the familiar object. Total time spent sniffing both objects was used as a measure of general exploration. Time spent sniffing two identical objects during the familiarization phase confirmed

the lack of an innate side bias. Objects utilized were plastic toys; a small soft plastic orange safety cone and a hard plastic conical magnetic with ribbed sides.

Open field activity: Exploratory locomotion was assessed in individual mice using an automated VersaMax Animal Activity Monitoring System (AccuScan Instruments, Columbus, OH) for a 30 minute test session under low light conditions (40 lux), as previously described (Brielmaier et al., 2012; Flannery et al., 2015; Kazdoba et al., 2016; Silverman et al., 2011).

Elevated plus-maze anxiety-related behavior: Subject mice were placed in the center area of a black Plexiglas automated elevated plus-maze (Med-Associates, St. Albans City, VT), under 300 lux white light illumination, for a 5 minute test session, as previously described (Brielmaier et al., 2012; Flannery et al., 2015; Kazdoba et al., 2016).

Light↔dark anxiety-related behavior: Subject mice were placed in the light side of a two-chambered light↔dark apparatus for a 10 minute session, as previously described (Flannery et al., 2015; Silverman et al., 2011). Time in the dark chamber and number of transitions between chambers were automatically recorded using Labview 8.5.1 (National Instruments, Austin, TX).

Statistical Analysis. Data were analyzed using Graphpad Prism version 5.0 (Graphpad, La Jolla, CA). For the Morris water maze, latency was analyzed using Two-Way Repeated Measures ANOVA with Bonferroni's post-hoc tests. Probe trial data were analyzed using One-Way ANOVA with Bonferroni post-tests. Novel object data were analyzed using paired Student's t-test. Open field activity data were analyzed by the Mann-Whitney test. Elevated plus-maze and light↔dark activity data were analyzed with unpaired t-tests with Welch's correction. Data are presented as mean ± SEM.

Supplemental References

Brielmaier, J., Matteson, P.G., Silverman, J.L., Senerth, J.M., Kelly, S., Genestine, M., Millonig, J.H., DiCicco-Bloom, E., and Crawley, J.N. (2012). Autism-relevant social abnormalities and cognitive deficits in engrailed-2 knockout mice. PLoS One *7*, e40914.

Flannery, B.M., Silverman, J.L., Bruun, D.A., Puhger, K.R., McCoy, M.R., Hammock, B.D., Crawley, J.N., and Lein, P.J. (2015). Behavioral assessment of NIH Swiss mice acutely intoxicated with tetramethylenedisulfotetramine. Neurotoxicol Teratol *47*, 36-45.

Kazdoba, T.M., Hagerman, R.J., Zolkowska, D., Rogawski, M.A., and Crawley, J.N. (2016). Evaluation of the neuroactive steroid ganaxolone on social and repetitive behaviors in the BTBR mouse model of autism. Psychopharmacology (Berl) *233*, 309-323.

Matt, L., Michalakis, S., Hofmann, F., Hammelmann, V., Ludwig, A., Biel, M., and Kleppisch, T. (2011). HCN2 channels in local inhibitory interneurons constrain LTP in the hippocampal direct perforant path. Cell Mol Life Sci *68*, 125-137.

Mattapallil, M.J., Wawrousek, E.F., Chan, C.C., Zhao, H., Roychoudhury, J., Ferguson, T.A., and Caspi, R.R. (2012). The Rd8 mutation of the Crb1 gene is present in vendor lines of C57BL/6N mice and embryonic stem cells, and confounds ocular induced mutant phenotypes. Invest Ophthalmol Vis Sci *53*, 2921-2927.

Priel, A., Kolleker, A., Ayalon, G., Gillor, M., Osten, P., and Stern-Bach, Y. (2005). Stargazin reduces desensitization and slows deactivation of the AMPA-type glutamate receptors. J Neurosci *25*, 2682-2686.

Priel, A., Selak, S., Lerma, J., and Stern-Bach, Y. (2006). Block of kainate receptor desensitization uncovers a key trafficking checkpoint. Neuron *52*, 1037-1046.

Silverman, J.L., Babineau, B.A., Oliver, C.F., Karras, M.N., and Crawley, J.N. (2013a). Influence of stimulant-induced hyperactivity on social approach in the BTBR mouse model of autism. Neuropharmacology *68*, 210-222.

Silverman, J.L., Oliver, C.F., Karras, M.N., Gastrell, P.T., and Crawley, J.N. (2013b). AMPAKINE enhancement of social interaction in the BTBR mouse model of autism. Neuropharmacology *64*, 268-282.

Silverman, J.L., Turner, S.M., Barkan, C.L., Tolu, S.S., Saxena, R., Hung, A.Y., Sheng, M., and Crawley, J.N. (2011). Sociability and motor functions in Shank1 mutant mice. Brain Res *1380*, 120-137.

Vorhees, C.V., and Williams, M.T. (2006). Morris water maze: procedures for assessing spatial and related forms of learning and memory. Nat Protoc *1*, 848-858.

Yang, M., Bozdagi, O., Scattoni, M.L., Wohr, M., Roullet, F.I., Katz, A.M., Abrams, D.N., Kalikhman, D., Simon, H., Woldeyohannes, L.*, et al.* (2012). Reduced excitatory neurotransmission and mild autism-relevant phenotypes in adolescent Shank3 null mutant mice. J Neurosci *32*, 6525-6541.